How to cite: *Angew. Chem. Int. Ed.* **2024**, *63*, e202406353
doi.org/10.1002/anie.202406353

Host-Guest Systems

Room-Temperature Near-Infrared Phosphorescence from C_{64} Nanographene Tetraimide by π-Stacking Complexation with Platinum Porphyrin

*M. A. Niyas, Swadhin Garain, Kazutaka Shoyama, and Frank Würthner**

Abstract: Near-Infrared (NIR) phosphorescence at room temperature is challenging to achieve for organic molecules due to negligible spin–orbit coupling and a low energy gap leading to fast non-radiative transitions. Here, we show a supramolecular host–guest strategy to harvest the energy from the low-lying triplet state of C_{64} nanographene tetraimide **1**. ^{1}H NMR and X-ray analysis confirmed the 1:2 stoichiometric binding of a Pt(II) porphyrin on the two π-surfaces of **1**. While the free **1** does not show emission in the NIR, the host–guest complex solution shows NIR phosphorescence at 77 K. Further, between 860–1100 nm, room temperature NIR phosphorescence (λ_{max} = 900 nm, τ_{avg} = 142 μs) was observed for a solid-state sample drop-casted from a preformed complex in solution. Theoretical calculations reveal a non-zero spin–orbit coupling between isoenergetic S_1 and T_3 of π-stacked [**1**·Pt(II) porphyrin] complex. External heavy-atom-induced spin–orbit coupling along with rigidification and protection from oxygen in the solid-state promotes both the intersystem crossing from the first excited singlet state into the triplet manifold and the NIR phosphorescence from the lowest triplet state of **1**.

Achieving room temperature phosphorescence (RTP) is challenging for organic molecules due to negligible spin–orbit coupling (SOC).[1] Strategies such as heavy-atom-effect,[2] crystallization,[3] and rigidification in a solid-state matrix[4] have been applied to harvest the triplet state of organic molecules in the visible region of the electromagnetic spectrum. However, RTP in the near-infrared region (NIR, 750–1700 nm) is still underexplored for organic molecules.[5] Owing to its applications in bioimaging,[6] night vision cameras and sensors,[7] NIR RTP is a highly sought after functional property. RTP in the NIR-II (1000–1700 nm) region is particularly suitable for bioimaging due to its low background autofluorescence, high spatial resolution, and deep tissue penetration.[6c,8] Although large π-conjugated polycyclic aromatic hydrocarbons (PAHs), i.e. nanographenes, have low-lying triplet energy levels, radiative NIR RTP has been barely observed for organic molecules.[9,5] This might be due to the lack of strategies to control intersystem crossing (ISC) and the radiative versus nonradiative decays of such molecules. Thus, the reported NIR phosphorescent emitters are almost exclusively coordination complexes of heavy-metals.[10] Motivated by previous reports on triplet harvesting through supramolecular interactions,[2a,c,3c,4b] and by our recent success in enhancing the fluorescence of a C_{54} nanographene tris(dicarboximide) by sequestration with hexabenzocoronene,[11] we hypothesized that large two-dimensional π-scaffolds with low-lying triplet states might also be sensitized for phosphorescence by means of the heavy-atom-effect exerted by neighbouring π-stacked platinum complexes that support the population of triplet states by interactions between Pt *d*-orbitals and π-orbitals of the nanographene, thereby promoting the radiative decay, i.e. NIR RTP, from the lowest triplet state of the nanographene.[2a,c,3b,4b]

Here we demonstrate such a supramolecular strategy for C_{64} nanographene tetraimide **1** (Figure 1a) being embedded between platinum complexes. Time dependent density functional theory (TDDFT) calculations suggest that **1** has a T_1 state at 938 nm which is spin forbidden and thus not emitting. However, as shown by ^{1}NMR and X-ray crystallographic analyses, **1** forms tightly stacked complex with platinum(II) 5,15-diphenylporphyrin **PtPor** (Figure 1b) which induces sufficient SOC to promote the desired NIR RTP of **1** with the help of molecular isolation and rigidification in the solid-state (Figure 1c).

C_{64} nanographene tetraimide **1** was synthesized by a cascade annulation reaction between pyrene tetraboronic acid pinacol tetraester and dibromonaphthalimide following our previously reported protocol.[12a] Owing to its large π-surface, **1** can bind a variety of PAHs as well as phthalocyanines on both π-surfaces to give 1:2 complexes.[12] Here we selected **PtPor** as the guest for stacking to **1** and inducing SOC by Pt···π interaction. Concentration-dependent UV/Vis spectra (Figure 2a) as well as ^{1}H NMR titrations (Figure S3) of **PtPor** with **1** in $CDCl_3$ showed changes in the absorption bands as well as the chemical shift in aromatic

[*] M. A. Niyas, Dr. S. Garain, Dr. K. Shoyama, Prof. Dr. F. Würthner
Institut für Organische Chemie, Universität Würzburg, Am Hubland, 97074 Würzburg, Germany
E-mail: frank.wuerthner@uni-wuerzburg.de
Dr. K. Shoyama, Prof. Dr. F. Würthner
Center for Nanosystems Chemistry (CNC), Universität Würzburg, Theodor-Boveri-Weg, 97074 Würzburg, Germany

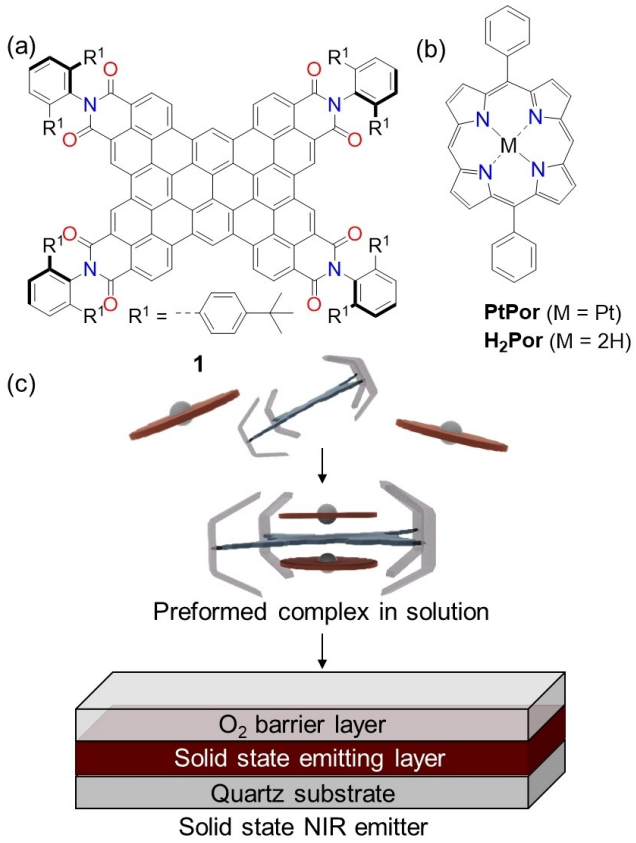

Figure 1. Chemical structures of (a) C_{64} nanographene tetraimide **1** and (b) porphyrin derivatives **PtPor** and **H_2Por**. (c) Graphical representation of our strategy to achieve NIR RTP. A preformed complex of **1** and **PtPor** is drop-casted on a quartz substrate and further coated with a transparent oxygen barrier layer to obtain NIR RTP.

protons of **1** indicating complexation. To understand the stoichiometry and mechanism of complexation, we performed an NMR titration at low temperature (195 K, CD_2Cl_2) to reach the regime of slow guest-exchange on the ^{1}H NMR time-scale. Slow exchange titration revealed a stepwise complexation from 1:1 to 1:2 stoichiometric complexes of **1** and **PtPor** (Figure S2). Further, X-ray crystallographic analysis of single crystals confirmed the thermodynamically favoured 1:2 stoichiometric complex of [**1**·2(**PtPor**)] (Figure 2b–d, Figure S1, Table S1). In this complex two equivalents of **PtPor** molecules are stacked on both sides of the π-surface of **1** aligned in a cross architecture with respect to each other. Pt(II) atoms are located in close van der Waals interaction range with the π-surface of **1** ($d_{Pt\cdots\pi}$ = 3.4–3.5 Å). Interactions between Pt and π-surface of **1** were also identified by observed electron density in the crystal structure indicating significant interaction in the crystalline state (Figure S1c). Once the structure was unambiguously confirmed, we went on to evaluate the association constants of **PtPor** and **H_2Por** with **1** from our ^{1}H NMR titration data at 295 K in $CDCl_3$. These binding constants and related Gibbs binding energies reveal a modest anti-cooperativity for binding of the two guests and, more importantly, a significantly higher binding constant for **PtPor** in comparison to **H_2Por** (Table 1). The former could be due to the structural change associated with first binding that leads to different orientation for the first and second binding as observed in X-ray crystal structure of [**1**·2(**PtPor**)] (Figure 2c,d). The latter we attribute to interactions between Pt *d*-orbitals and the π-cloud of **1** in addition to the π–π-interactions (mostly London dispersion) between the π-scaffolds of **1** and porphyrin in the [**1**·2(**PtPor**)] complex.

Nanographene **1** shows fluorescence in toluene between 600–850 nm with an emission maximum at 603 nm. **1** exhibits a fluorescence quantum yield of 71 % in toluene (Figure S5, Table S2). Change in photoluminescence due to supramolecular complexation was assessed by a fluorescence titration of **1** with **PtPor** at low concentration (c(**1**) ≈ 10^{-7} M) in CCl_4 owing to the higher binding constants in this solvent ($K_1 \approx 10^6$ M^{-1}, $K_2 \approx 10^4$ M^{-1}). Titration of 8 equiv-

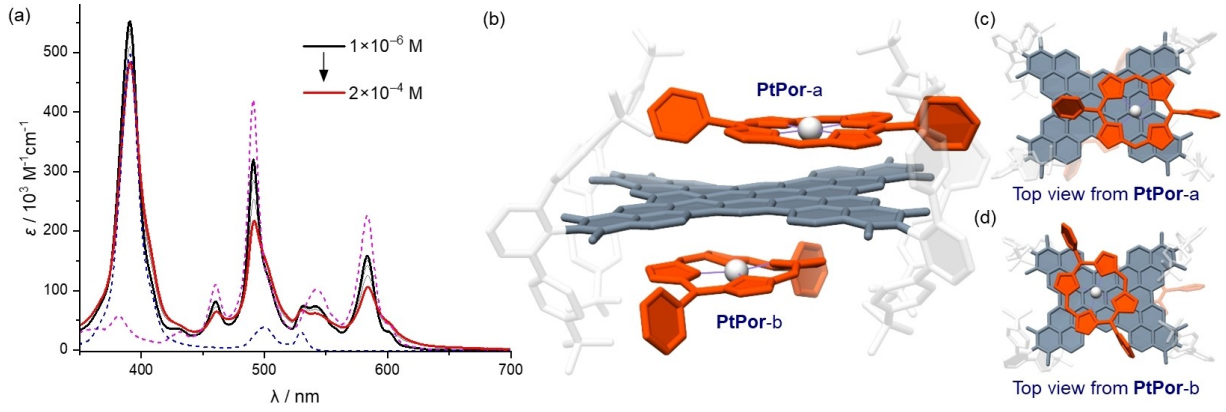

Figure 2. (a) Concentration-dependent UV/Vis absorption spectra of the 1:2 stoichiometric [**1**·2(**PtPor**)] complex in toluene (red and black lines for the indicated concentrations). The changes in absorbance on increasing concentration show the complexation. Magenta dotted spectra corresponds to monomeric **1** in toluene (c(**1**) = 1×10^{-6} M) and blue dotted spectra corresponds to monomeric **PtPor** in toluene (c(**PtPor**) = 2×10^{-6} M). (b) X-ray crystal structure of [**1**·2(**PtPor**)] supramolecular complex. Two **PtPor** molecules are π-stacked in different orientations with respect to each other in the crystalline state. Top view from (c) **PtPor**-a and (d) **PtPor**-b are shown.

Table 1: Association parameters for the complexation of **1** with **PtPor** and **H_2Por** in $CDCl_3$ at 295 K.

Guest	K_1 (M^{-1})[a]	K_2 (M^{-1})[a]	ΔG_1[b] (kJ mol^{-1})	ΔG_2[b] (kJ mol^{-1})
PtPor	1.2×10^5	1.4×10^3	−28.8	−17.8
H_2Por	1.9×10^4	1.2×10^3	−24.2	−17.4

[a] Association constants K_1 and K_2 determined from ^{1}H NMR titration data with the program bindfit[13] for a 1:2 binding model in $CDCl_3$. [b] Gibbs free energies ΔG_1 and ΔG_2 (295 K) calculated from K_1 and K_2 according to $\Delta G(295\ K) = -RT\ln(K)$. Experimental details, fitting plots, and errors are given in the Supporting Information.

alents (affording 90 % complexation) of **PtPor** showed a decrease of the fluorescence quantum yield from 53 % to 26 % in CCl_4 and no additional phosphorescence was observed at longer wavelengths (Figure S6). Similar to CCl_4, no emission at the NIR range was observed for a complex solution in toluene at 295 K (c(**1**) = 1.5×10^{-4} M, c(**PtPor**) = 2×c(**1**), Figure S7). However, when we froze the solution to 77 K, we observed a new band between 860–1100 nm (Figure S7). With a lifetime of τ_{avg} = 439 µs (Table S3) this new band can be assigned as phosphorescence. No such long-lived NIR emission was observed when we measured a frozen glass of corresponding free base (without platinum) derivative, [**1**·2(**H_2Por**)], in toluene. As **PtPor** by itself does not emit above 850 nm, we attribute the new band to the triplet emission of **1**. For further clarification whether the phosphorescence band in the NIR originates from the triplet state of **1** or from a charge transfer state involving both **PtPor** and **1** we prepared a solution of **1** with excess of platinum (II) acetylacetonate ($Pt(acac)_2$). Indeed, a large excess of $Pt(acac)_2$ with **1** afforded the same emission in frozen glass between 850–1100 nm (λ_{max} = 880 nm) with a microsecond lifetime (τ_{avg} = 407 µs, Figure S8, Table S4). This verifies that the structured emission observed between 860–1100 nm is phosphorescence from the triplet state of **1**.

RTP is a highly sought after functional property which is rarely observed for NIR emitters. Reducing the access of oxygen and ISC-promoting molecular vibrations of the triplet excited emitter molecule by solidification is a common strategy to achieve RTP. Once we knew that the T_1 state of **1** could be activated to give phosphorescence by complexation in frozen solution, we hypothesized that a preformed complex in solution could be solidified to make an NIR RTP material. Thus, we prepared a 1:2 stoichiometric solution of **1** and **PtPor** in 0.2 mL CH_2Cl_2 (c(**1**) = 6×10^{-4} M) and drop-casted it on a quartz substrate and allowed to dry. Upon excitation at 550 nm, we observed an emission of very low intensity at 900 nm (Figure S9). We then coated the drop-casted substrate with a layer of polyvinyl alcohol (PVA) as an oxygen barrier material to improve the emission intensity. PVA is water soluble and does not interact with the drop-casted complexes as both **1** and **PtPor** are insoluble in water. After coating with PVA, the emission intensity increased almost 20 times and displayed a structured band (860–1100 nm) with a maximum at 900 nm and a shoulder at 1030 nm (λ_{exc} = 550 nm, Figure 3a,

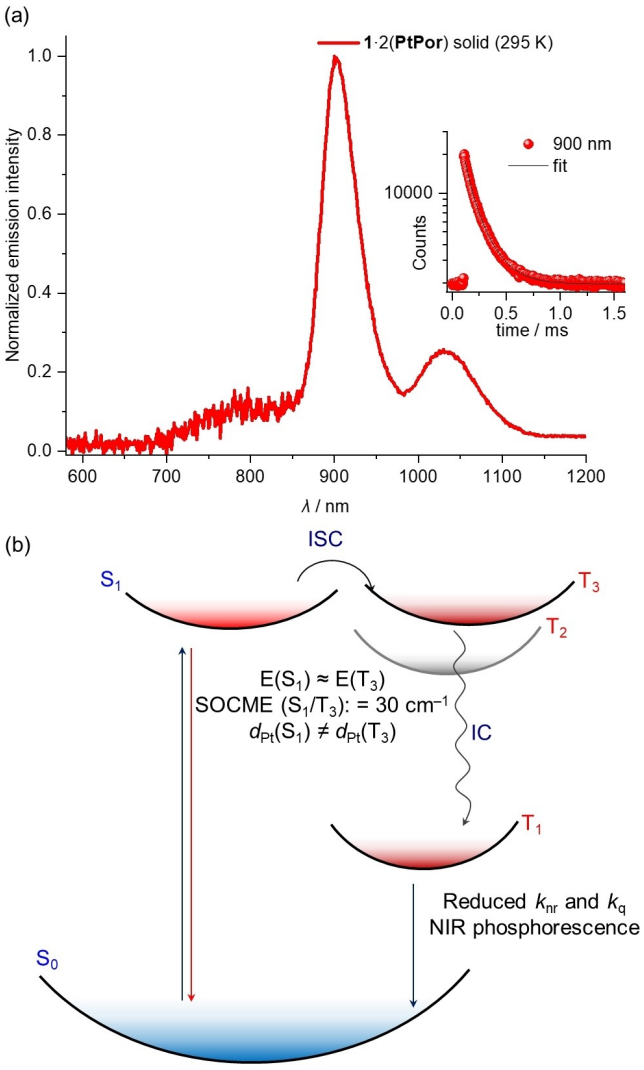

Figure 3. (a) Emission spectra (λ_{exc} = 550 nm) showing NIR RTP from a drop-casted solid-state sample of [**1**·2(**PtPor**)] coated with PVA oxygen barrier layer. Inset shows the lifetime decay of the phosphorescence. (b) Excited states energy level diagram showing the excited state dynamics leading to NIR phosphorescence in [**1**·2(**PtPor**)] complex. Solidification leads to a reduced non-radiative rate (k_{nr}) and the barrier layer suppresses the triplet quenching (k_q) by oxygen.

Figure S9). Lifetime analysis confirmed that the emission in the NIR range originated from a triplet state (τ_{avg} = 142 µs, Table S5). With an integrating sphere an absolute quantum yield of (0.12 ± 0.02) % was determined for the NIR RTP (Figure S12). Furthermore, upon cooling the solid sample down to 77 K, an increase in intensity and lifetime of the NIR emission was observed (Figure S10). Choosing rigid side chains on both **1** and Pt(II) porphyrin guest or by choosing a Pt(II) complex with higher association strength could improve the quantum yield for NIR RTP.

Efficient population of the triplet manifold typically requires triplet states that are energetically close to the S_1 state and that are coupled by sufficiently large spin–orbit coupling matrix elements (SOCME).[1b,14] To get insight into the mechanistic pathway for the [**1**·2(**PtPor**)] complex, we

performed TDDFT and SOCME calculations for the excited states (details of theoretical methods are given in the Supporting Information). Based on these calculations we propose a pathway of initial fast relaxation of the excited complex to the lowest energy S_1 state via internal conversion (Kasha's rule).[15] Due to the significant charge transfer character of S_1 with **PtPor** acting as a donor and **1** as an acceptor, there is non-zero SOCME to the triplet states that are energetically below this singlet state (Figure 3b, Figure S13). Calculated SOCMEs between S_1/T_1, S_1/T_2 and S_1/T_3 are indeed all around 20–30 cm^{-1} due to a similar impact of the co-facially stacked Pt on the various π-orbitals of **1** (Table S6). The SOCME values realised by the intermolecular contact in the π-stack are not particularly high but agree well with the observed low NIR RTP quantum yield. Non-radiative decay rate (k_{nr}) and triplet quenching (k_q) are partially suppressed by the rigidification in the solid-state and oxygen barrier layer, respectively. This nevertheless demonstrates the general applicability of our approach of utilizing π-stacked complexes of heavy-metal containing molecules for the sensitization of phosphorescence of aromatic dicarboximides in the solid-state.[2a] Visualizing the natural transition orbitals (NTOs) further reveals that the ISC between S_1 and T_3 involves a change in Pt *d*-orbital character which is required for efficient ISC according to El-Sayed's rule[16] (Figure S13b). Thus, considering the requirement of isoenergetic states and El-Sayed's rule, we propose that in our complex the ISC proceeds from S_1 to T_3 state, followed by a fast internal conversion (IC) to T_1. Because T_1 (different from S_0) has a local excitation character, the following radiative transition (phosphorescence) from T_1 to S_0 originates from the heavy-metal-free nanographene tetraimide **1** (Figure S13a). Thus, via a supramolecular interaction between **PtPor** and **1** in a tightly stacked complex, the phosphorescence of **1** in the NIR region could be sensitized in the solid-state.

In conclusion, we demonstrated how an RTP emission in the NIR region can be sensitized for nanographene tetraimide **1** by a tailored supramolecular matrix consisting of co-facially stacked Pt complexes such as **PtPor** or $Pt(acac)_2$. To demonstrate this concept, the large π-surface of **1** was crucial as it provides a sufficiently large surface for binding **PtPor** molecules in a 1:2 stoichiometric supramolecular complex already in dilute solution. Upon drop-casting this pre-assembled complex onto a quartz substrate and coating it with an oxygen barrier layer, NIR RTP could be realised. This result could be explained by the external heavy-atom-induced SOC originating from the interaction of Pt with π-orbitals of **1**, leading to ISC and phosphorescence assisted by isolation from triplet quenching by oxygen and rigidification in the solid-state. Due to the large two-dimensional π-system of **1**, NIR RTP extends into the NIR-II region (860–1010 nm) with an average lifetime of 142 μs. Our work shows that supramolecular matrices can be tailored to exert desirable external heavy-atom-effects. We expect that any square planar Pt(II) salt or Pt(II) complex that forms π-stacked complex with C_{64} nanographene would sensitize the triplet state via external heavy-atom-induced ISC. We consider this approach to be quite general and envision a plethora of recently synthesized nanographenes[17] and molecular carbon multiimides[18] to be applicable as visible/NIR phosphorescent emitters upon π-stacking complexation with suitable square-planar platinum compounds.

Acknowledgements

We thank the Deutsche Forschungsgemeinschaft (DFG, German Research Foundation) for financial support (grant no. WU 317/20-2). We acknowledge DESY (Hamburg, Germany), a member of the Helmholtz Association HGF, for the provision of experimental facilities. Parts of this research were carried out at PETRA III and we would like to thank Dr. Johanna Hakanpää for assistance in using P11. Beamtime was allocated for proposal I-20230262. We thank Dr. Menyhárt Sárosi for the insightful discussions on the theoretical calculations. Open Access funding enabled and organized by Projekt DEAL.

Conflict of Interest

The authors declare no conflict of interest.

Data Availability Statement

X-ray crystallographic data are available free of charge from the Cambridge Crystallographic Data Centre under the reference numbers CCDC 2331508 via https://www.ccdc.cam.ac.uk/structures/. Additional data supporting the findings are contained in the main text or the Supporting Information. All source files are openly available in Zenodo at https://doi.org/10.5281/zenodo.10878594.

Keywords: Host–guest systems · Nanographene · Phosphorescence · Supramolecular Chemistry · Photochemistry

[1] a) S. Hirata, *Adv. Opt. Mater.* **2017**, *5*, 1700116; b) D. Sasikumar, A. T. John, J. Sunny, M. Hariharan, *Chem. Soc. Rev.* **2020**, *49*, 6122–6140.

[2] a) M. J. Sun, O. Anhalt, M. B. Sárosi, M. Stolte, F. Würthner, *Adv. Mater.* **2022**, *34*, 2207331; b) A. V. Rozhkov, I. V. Ananyev, R. M. Gomila, A. Frontera, V. Y. Kukushkin, *Inorg. Chem.* **2020**, *59*, 9308–9314; c) S. Garain, S. Kuila, B. C. Garain, M. Kataria, A. Borah, S. K. Pati, S. J. George, *Angew. Chem. Int. Ed.* **2021**, *60*, 12323–12327; *Angew. Chem.* **2021**, *133*, 12431–12435.

[3] a) E. Hamzehpoor, D. F. Perepichka, *Angew. Chem. Int. Ed.* **2020**, *59*, 9977–9981; *Angew. Chem.* **2020**, *132*, 10063–10067; b) M. Singh, K. Liu, S. Qu, H. Ma, H. Shi, Z. An, W. Huang, *Adv. Opt. Mater.* **2021**, *9*, 2002197; c) O. Bolton, K. Lee, H. J. Kim, K. Y. Lin, J. Kim, *Nat. Chem.* **2011**, *3*, 205–210; d) A. D. Nidhankar, Goudappagouda, D. S. M. Kumari, S. K. Chaubey, R. Nayak, R. G. Gonnade, G. V. P. Kumar, R. Krishnan, S. S. Babu, *Angew. Chem. Int. Ed.* **2020**, *59*, 13079–13085; *Angew. Chem.* **2020**, *132*, 13179–13185; e) K. Vinod, S. D. Jadhav, M. Hariharan, *Chem. A Eur. J.* **2024**, e202400499.

[4] a) X. Fu, H. Jin, Z. Ma, X. Zhang, C. Qian, Z. Li, Z. Chi, Z. Ma, *ACS Appl. Mater. Interfaces* **2023**, *15*, 30804–30814; b) W. Zhao, Z. He, B. Z. Tang, *Nat. Rev. Mater.* **2020**, *5*, 869–885; c) S. Hirata, K. Totani, J. Zhang, T. Yamashita, H. Kaji, S. R. Marder, T. Watanabe, C. Adachi, *Adv. Funct. Mater.* **2013**, *23*, 3386–3397; d) M. S. Kwon, Y. Yu, C. Coburn, A. W. Phillips, K. Chung, A. Shanker, J. Jung, G. Kim, K. Pipe, S. R. Forrest, J. H. Youk, J. Gierschner, J. Kim, *Nat. Commun.* **2015**, *6*, 8947; e) S. Kuila, K. V. Rao, S. Garain, P. K. Samanta, S. Das, S. K. Pati, M. Eswaramoorthy, S. J. George, *Angew. Chem. Int. Ed.* **2018**, *57*, 17115–17119; *Angew. Chem.* **2018**, *130*, 17361–17365.

[5] F. Xiao, H. Gao, Y. Lei, W. Dai, M. Liu, X. Zheng, Z. Cai, X. Huang, H. Wu, D. Ding, *Nat. Commun.* **2022**, *13*, 186.

[6] a) V. J. Pansare, S. Hejazi, W. J. Faenza, R. K. Prud'homme, *Chem. Mater.* **2012**, *24*, 812–827; b) G. Hong, A. L. Antaris, H. Dai, *Nat. Biomed. Eng.* **2017**, *1*, 0010; c) B. Chang, J. Chen, J. Bao, T. Sun, Z. Cheng, *Chem. Rev.* **2023**, *123*, 13966–14037; d) C. Li, G. Chen, Y. Zhang, F. Wu, Q. Wang, *J. Am. Chem. Soc.* **2020**, *142*, 14789–14804.

[7] a) N. Tessler, V. Medvedev, M. Kazes, S. Kan, U. Banin, *Science* **2002**, *295*, 1506–1508; b) G. Qian, Z. Y. Wang, *Chem. Asian J.* **2010**, *5*, 1006–1029; c) Y. Xiao, H. Wang, Z. Xie, M. Shen, R. Huang, Y. Miao, G. Liu, T. Yu, W. Huang, *Chem. Sci.* **2022**, *13*, 8906–8923; d) M. Villa, B. D. Secco, L. Ravotto, M. Roy, E. Rampazzo, N. Zaccheroni, L. Prodi, M. Gingras, S. A. Vinogradov, P. Ceroni, *J. Phys. Chem. C* **2019**, *123*, 29884–29890.

[8] Z. Feng, T. Tang, T. Wu, X. Yu, Y. Zhang, M. Wang, J. Zheng, Y. Ying, S. Chen, J. Zhou, X. Fan, D. Zhang, S. Li, M. Zhang, J. Qian, *Light-Sci. Appl.* **2021**, *10*, 197.

[9] D. Lee, X. Ma, J. Jung, E. J. Jeong, H. Hashemi, A. Bregman, J. Kieffer, J. Kim, *Phys. Chem. Chem. Phys.* **2015**, *17*, 19096–19103.

[10] a) J. R. Sommer, A. H. Shelton, A. Parthasarathy, I. Ghiviriga, J. R. Reynolds, K. S. Schanze, *Chem. Mater.* **2011**, *23*, 5296–5304; b) H. Xiang, J. Cheng, X. Ma, X. Zhou, J. J. Chruma, *Chem. Soc. Rev.* **2013**, *42*, 6128–6185; c) K. Li, G. S. M. Tong, Q. Wan, G. Cheng, W.-Y. Tong, W.-H. Ang, W.-L. Kwong, C.-M. Che, *Chem. Sci.* **2015**, *7*, 1653–1673; d) V. W.-W. Yam, V. K.-M. Au, S. Y.-L. Leung, *Chem. Rev.* **2015**, *115*, 7589–7728; e) Y. Zhang, Y. Wang, J. Song, J. Qu, B. Li, W. Zhu, W. Y. Wong, *Adv. Opt. Mater.* **2018**, *6*, 1800466; f) T. Theiss, S. Buss, I. Maisuls, R. López-Arteaga, D. Brünink, J. Kösters, A. Hepp, N. L. Doltsinis, E. A. Weiss, C. A. Strassert, *J. Am. Chem. Soc.* **2023**, *145*, 3937–3951.

[11] B. Pigulski, K. Shoyama, M.-J. Sun, F. Würthner, *J. Am. Chem. Soc.* **2022**, *144*, 5718–5722.

[12] a) M. Mahl, M. A. Niyas, K. Shoyama, F. Würthner, *Nat. Chem.* **2022**, *14*, 457–462; b) M. A. Niyas, K. Shoyama, F. Würthner, *Angew. Chem. Int. Ed.* **2023**, *62*, e202302032; *Angew. Chem.* **2023**, *135*, e202302032.

[13] a) D. B. Hibbert, P. Thordarson, *Chem. Commun.* **2016**, *52*, 12792–12805; b) P. Thordarson, *Chem. Soc. Rev.* **2011**, *40*, 1305–1323.

[14] T. J. Penfold, E. Gindensperger, C. Daniel, C. M. Marian, *Chem. Rev.* **2018**, *118*, 6975–7025.

[15] M. Kasha, *Discuss. Faraday Soc.* **1950**, *9*, 14–19.

[16] S. K. Lower, M. A. El-Sayed, *Chem. Rev.* **1966**, *66*, 199–241.

[17] L. Chen, Y. Hernandez, X. Feng, K. Müllen, *Angew. Chem. Int. Ed.* **2012**, *51*, 7640–7654; *Angew. Chem.* **2012**, *124*, 7758–7773.

[18] W. Jiang, Z. Wang, *J. Am. Chem. Soc.* **2022**, *144*, 14976–14991.

Manuscript received: April 3, 2024
Accepted manuscript online: May 7, 2024
Version of record online: June 14, 2024